Dual-Frequency Altimetry: What have we learnt from Envisat RA-2's S-band?

G.D. Quartly[1], J. Gómez-Enri[1], A. Caltabiano[1] & D.J.T. Carter[2]

1 - Southampton Oceanography Centre,
2 - Satellite Observing Systems

gdq@soc.soton.ac.uk

Introduction

Many satellite altimeters have operated at K_u-band (around 13.6 GHz, corresponding to a wavelength of 2.2 cm). As the ionospheric delay is proportional to the square of the frequency, recent altimeters have incorporated a second frequency to help recover this correction. With TOPEX and Jason, this secondary frequency is at C-band (5.3 GHz, eqv. to 5.7 cm); with Envisat's RA-2 it is at S-band (3.2 GHz, eqv. to 9.4 cm). The European Space Agency has supported a **RAIES** project (**Radar Altimeter Individual Echoes and S-band**) based at Southampton Oceanography Centre; this poster covers only that portion of the work relating to S-band. Here, using a combination of waveform simulations and data intercomparisons, we look at the added information gained from the S-band values of range, wave height and backscatter.

RA-2 Waveforms

The K_u-band operation of RA-2 generates ~1800 pulses per second, and records the average of groups of 100, discretizing the information as 128 bins of width 3.125 ns; each bin thus corresponds to a two-way range of 46.9 cm. The operation at S-band is similar, except that there are 450 pulses per second, averaged in groups of 25, and that the collected data is averaged pairwise before transmission to give 64 bins of width 6.25 ns. From these average waveforms a number of parameters can be deduced — the key three are:

- position of the half-power point (related to range)
- the slope of the leading edge (related to wave height, H_s)
- the amplitude (normalized backscatter strength, σ^0, related to surface roughness)

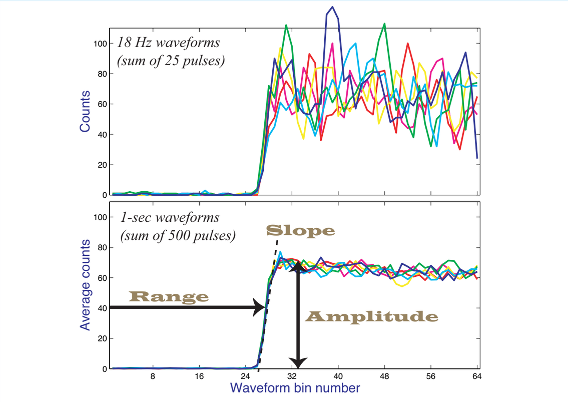

Upper plot: 6 consecutive 18 Hz waveforms from RA-2 S-band. Lower plot: 6 consecutive 1-sec averages.

Over the ocean, σ^0 is principally dependent upon wind speed, but rain can have a major effect. Waveforms over non-ocean surfaces are more much more complicated to interpret; here, the only non-marine work concerns σ^0 values over Antarctica.

The S-band determinations of range, wave height and σ^0 are assessed by comparison with other data sources or model output. Some insight into performance is also given by simulating the S-band waveforms as telemetered from Envisat, and also with a greater number of pulses or narrower bins to see whether these operational choices have affected performance.

Waveform Simulation and Retracking

We have simulated waveforms using the formulation of Challenor & Srokosz (1989), and applied Rayleigh (fading) noise; parameters are then estimated using Maximum Likelihood Estimation. We simulate three S-band operating scenarios:

- **Original** (25 pulses; 6.25 ns width bins)
- **High PRF** (100 pulses; 6.25 ns width bins)
- **Fine res.** (25 pulses; 3.125 ns width bins)
- **K_u-like** (100 pulses; 3.125 ns width bins)

Results shown are for 18 Hz waveforms, not 1-sec averages.

Ionospheric delay (Track point)

The difference between the K_u- and S-band track point is used to calculate the ionospheric correction at each frequency.

$$\Delta_{iono\,(Ku)} = \frac{40.3\ TEC}{f^2_{Ku}} \quad + \quad \Delta_{iono\,(S)} = \frac{40.3\ TEC}{f^2_{S}} \quad \rightarrow \quad \Delta_{iono\,(Ku)} = \Delta h \frac{f^2_{S}}{f^2_{Ku} - f^2_{S}}$$

where f_{Ku} and f_S are the frequencies of K_u- and S-band, TEC is the unknown Total Electron Content and Δh is the difference in the two track points due to the differing ionospheric delays, assuming no other correction is frequency dependent.

The derived corrections are compared with values derived from JPL's Global Ionospheric Model. The best fit line through the data is:

$\Delta iono_{\,(dual\text{-}freq)} = \Delta iono_{\,(GIM)} * 0.97 + 0.5$ cm, with a scatter of 1.3 cm (r^2=0.85).

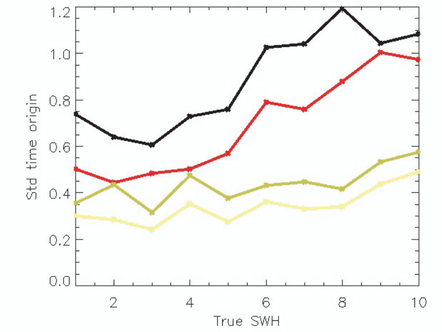

R.m.s. variability of tracker point with H_s, for different scenarios of S-band operation (see left hand panel of poster)

Simulations show that significant improvements could be made by increasing the number of pulses, and halving the bin size. However, the effect on the required correction is minor, being only 6% of variability in S-band tracker point (see equations above). Also, in a global sense, the present error is small anyway.

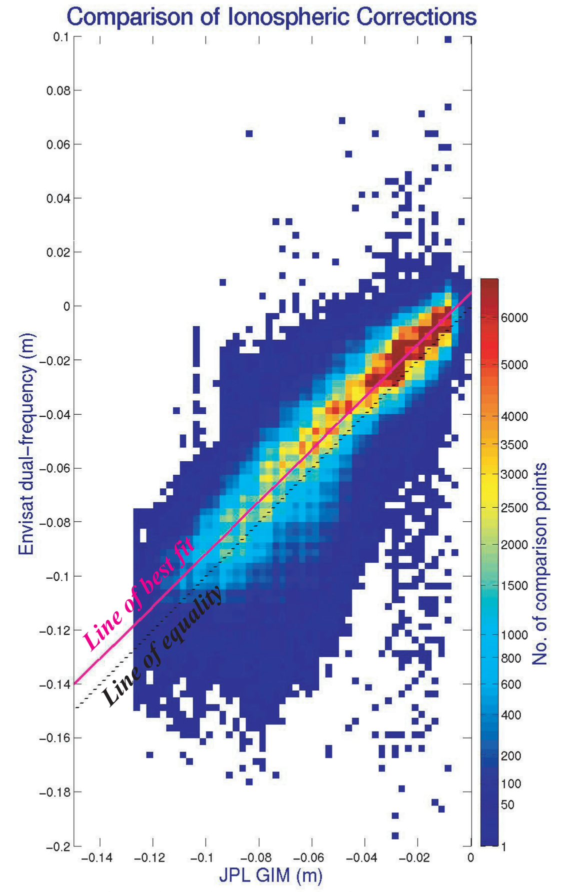

Scatter plot of 2 independent estimates of ionospheric corrections. (Altimeter data are from RA-2 cycle 25, with careful screening to remove land, rain and sea-ice; model data are from JPL's Global Ionospheric Model.)

Sigma0, σ^0

The accuracy of sigma0 estimates does depend upon the simulation conditions (more pulses leads to improved accuracy), but in all cases the error is small compared to that required for geophysical applications.

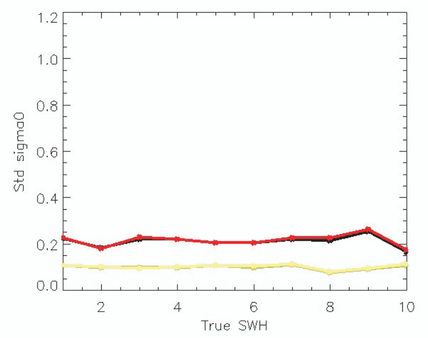

Variability of tracker point (in ns) for different simulation scenarios (see left hand panel of poster)

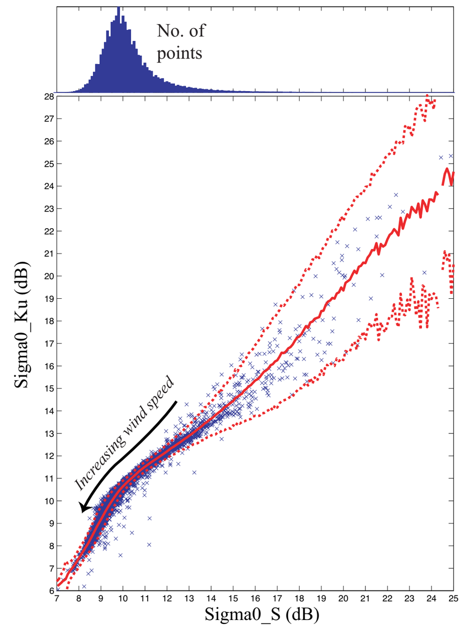

Scatter plot of simultaneous σ^0_{Ku} and σ^0_S observations over the ocean

There is clearly a very close correspondence between σ^0_S and σ^0_{Ku}, although the effect is not linear. The two wavelengths of radiation interact with the sea surface at different roughness scales; higher winds increase roughness at all scales, but around 7 m/s (the mode of the histogram) the scales pertinent to S-band are increased proportionately more, with the smaller wavelengths that interact with K_u-band having an increased response at a higher wind speed.

By looking at σ^0_{Ku} - σ^0_S we can see this in fine detail and note how the correspondence varies with H_s. Points lying significantly below the mean relationship can usually be attributed to rain (if neither land nor sea-ice are present). However, the wide scatter at low wind speed (high σ^0) and the sensitivity to H_s necessitate extra editing, either using Liquid Water Content from the microwave radiometer or a cut-off at high σ^0.

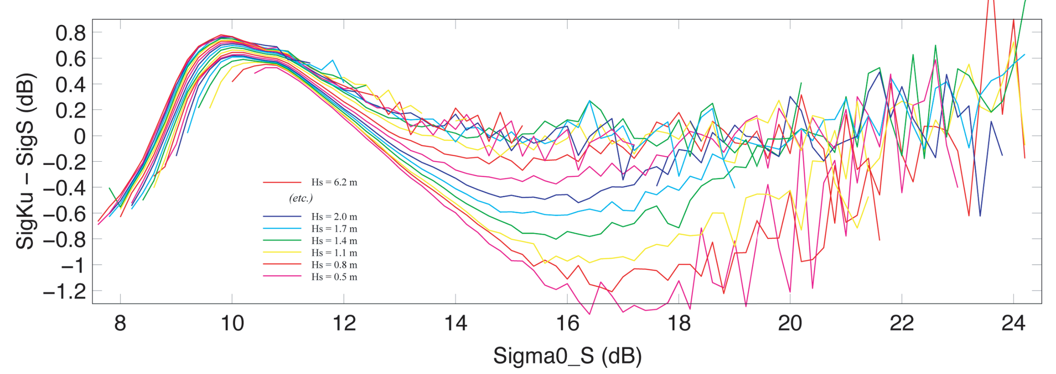

Mean relationship between backscatter at S-band and K_u-band as a function of wave height

An extension is to combine fine-scale altimetric rain detection with information from other Envisat sensors (see poster G27 by Quartly & Poulsen in *Science Plans and Results*).

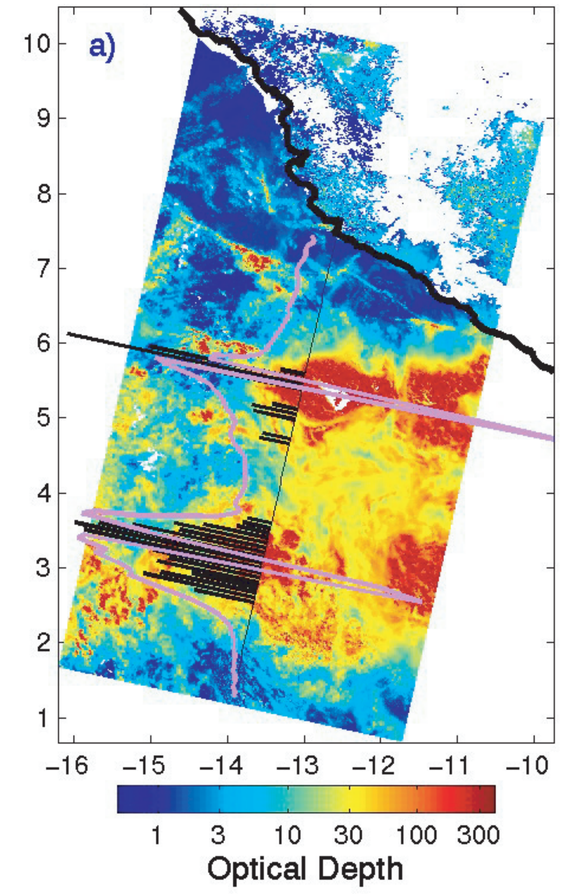

Multi-sensor observation of raining cloud off W. Africa. Optical depth (in colour) is from AATSR, rain rate (blck bars) is from RA-2 & Liquid Water Content (pink line) is from MWR

Conclusions

The S-band altimeter was designed with a lower pulse repetition frequency (PRF) than K_u-band, and with wider bins. This affects the recovery of the track point, but the effect on ionospheric correction is small. Wave height is determined from the derivative of the waveform; the choice of low PRF and double-width bins explains much of why S-band estimates of H_s are poor.

The backscatter, σ^0, is an integrated quantity, and so less sensitive to the choice of operating scenario. Comparisons of ocean values of σ^0_S and σ^0_{Ku} show:

- a close correspondence
- a dependence upon H_s, showing how wave height affects sea surface roughness
- a means of rain detection (Quartly & Srokosz, 2003; Tournadre, 2004) that can be combined with other Envisat sensors for synergistic studies of rain clouds (Quartly & Poulsen, 2004)
- a mean of editing altimetric data to remove effect of rain, ice and S-band anomalies (Lillibridge et al., 2004)

Applications over land surface are still to be developed, but the properties over the ice plateaux seem very stable.

References

Challenor P.G. and M.A. Srokosz, 1989, The extraction of geophysical parameters from radar altimeter returns from a non-linear sea surface, In Mathematics in Remote Sensing, Clarendon press, Oxford.

Lillibridge, J., R. Scharroo and G. Quartly, 2004, Rain and ice flagging of Envisat altimeter and MWR data, Proceedings of Envisat symposium, Salzburg, 6-10th Oct. 2004 (8pp).

Quartly, G.D. and C.A. Poulsen, 2004, Coincident cloud observations by altimetry and radiometry, Proceedings of Envisat symposium, Salzburg, 6-10th Oct. 2004 (5pp).

Quartly G.D. and M.A. Srokosz, 2003, Rain-flagging of the Envisat altimeter, Proc. of IGARSS 2003 21st-25th July 2003, Toulouse, France (3pp)

Tournadre, J., 2004, Validation of Jason and Envisat dual frequency rain flags, Marine Geodesy. 27 (1-2), 153-169.

Wave Height

To assess the quality of S-band estimates of wave height, H_s, we need a reference source of data. Given the limited number of RA-2 overpasses of buoys to-date, we instead use a triple collocation involving Envisat's K_u- and S-band measurement and ERS-2 (which follows the same path 29 minutes later). Comparisons may then be done using each of the three pairs of datasets (see illustration).

Minimum distance regression using RA-2's two sets of H_s values shows the S-band to read lower for wave heights below 2m, but higher for large wave heights. There is also a significant amount of scatter about the fitted line, with r^2 being 0.830. This improves after application of a 5-point running mean filter (r^2=0.943). However, the comparison between K_u-band and ERS-2 (29 minutes part) is much better, with a slope close to unity.

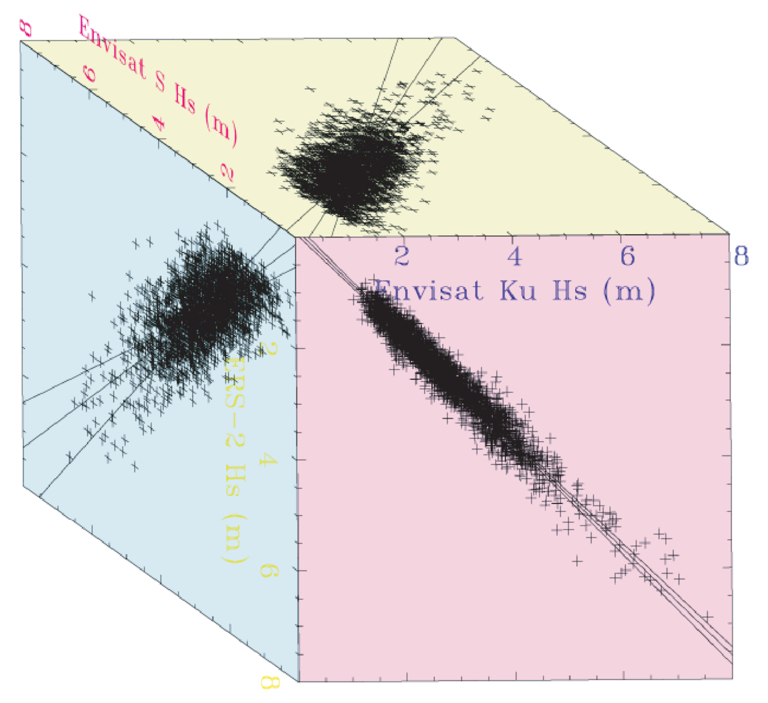

Application of triple regression analysis (P. Challenor, pers. comm.) shows the residual standard deviation of S-band wave heights to be 4.2 times those at K_u-band. It had been hoped that S-band values would prove more useful than K_u across severe storms (where attenuation by rain affects the waveforms); however, analysis of extreme events showed this not to be the case on average.

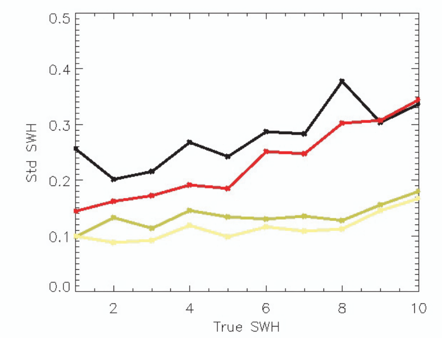

Variability of wave height estimate for different simulation scenarios (see left hand panel of poster)

Retracking of simulated waveforms indicate that the number of S-band pulses relative to K_u only explains a factor of 2 in the ratio of standard deviations, and that halving the bin size would only make a slight improvement (except for at low wave heights, where the effect is more pronounced).

Backscatter, σ^0, over ice

Typical σ^0_{Ku} values over Antarctica are around 4-10 dB i.e. weaker returns than over most of the ocean. The values represent the effects of both surface and volume scattering, which will differ at the two frequencies.

Circumference — Plots of σ^0_{Ku} - σ^0_S around South Pole for RA-2 cycles 15 to 24. The mean value for each ocean location is close to zero, whilst that for sea-ice is high. Note the stability of the patterns within the Antarctic plateau, where the σ^0_{Ku} values are 2-3 dB more than the σ^0_S values but that offset remains constant throughout the year. (An offset of 0.68 dB is applied to σ^0_S values from cycle 22 onwards.)

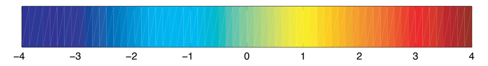

Sigma0_Ku - Sigma0_S (dB)

Centre — Plot of r.m.s. variability of σ^0_{Ku}-σ^0_S, showing regions of great constancy. Contours indicate heights of 0, 2 and 3 km above sea level.

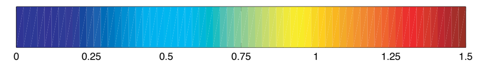

Variability of Sigma0_Ku - Sigma0_S (dB)